Journal of Network Computing and Applications (2024)
Clausius Scientific Press, Canada

DOI: 10.23977/jnca.2024.090103
ISSN 2371-9214 Vol. 9 Num. 1

Research on the Coverage Width and Overlap Rate of Seabed Topography Based on Multibeam Sonar

Junsong Yu[1,*], Fangxv Lou[1], Rongrong Fu[2], Wei Luo[1], Jianwei Wang[1,*]

[1]*School of Big Data and Computer Science, Guizhou Normal University, Guiyang, 550025, China*
[2]*School of Foreign Languages, Guizhou Normal University, Guiyang, 550025, China*
[*]*Corresponding author: dennisfeather@126.com*

Keywords: Multi-beam Measurements, Overlap Rate, Geometric Model, Coverage Width

Abstract: This paper proposes a novel physical calculation model for analyzing coverage rates and areas in multibeam sonar technology, focusing on the impact of transducer opening angles and seabed slope variations. The model addresses coverage width issues and the overlap rates between adjacent strips, demonstrating that a coverage width of 243.07 meters results in a 20.49% overlap, while a width of 224.88 meters yields a 14.31% overlap. Additionally, a method for calculating coverage width in rectangular sea areas is introduced, facilitating efficient sonar coverage and overlap rate analysis. The research enriches multibeam sounding systems and provides insights into elliptical coverage areas based on varying angles between survey lines. For instance, with a distance of 1.5 nautical miles from the survey vessel to the center of the sea area and a 90-degree angle between survey lines, the coverage width is 416.69 meters.

1. Introduction

The oceans, which cover 71% of the global area, harbor extremely rich biological and mineral resources, which are vital for economic development. Scientific understanding and efficient development and utilization of the oceans are beneficial for countries to safeguard their maritime rights and interests and to achieve sustainable development. Bathymetric mapping of the seabed is a precursor to all marine activities such as ocean development, fisheries monitoring, environmental protection, and military activities, and it has significant research importance.

Multibeam echo sounders are a new method for the development of marine underwater resources. Compared with the traditional single-beam echo-sounding technology, it has the characteristics of a wide scan width, full coverage, high efficiency, and high precision, which greatly improve the efficiency of mapping work. The principle is to use a transducer to emit sound waves to the seabed, and the receiving transducer receives the reflected echo signals. Then, based on the reception time and sound speed, the water depth can be calculated, thereby reliably depicting the three-dimensional characteristics of the seabed topography.

Therefore, this paper processes the three-dimensional characteristics of the seabed terrain data obtained by the multi-beam sounding system. It addresses the coverage width and overlap rate between adjacent strips of multi-beam measurement through physical modeling. At the same time, it provides a method for the coverage width of multi-beam sounding in the case of a rectangular sea

area, which has a certain reference value for the multi-beam sounding system on the seabed[1-4].

2. Analysis of Acoustic Coverage and Overlap Rate in Seabed Mapping

The seabed baseline is typically complex. To simplify the research, this study projects the cross-section of the sound wave emitted by the multi-beam transducer onto the sea surface, forming an isosceles triangle with the intersection line of the seabed slope, which adapts to various terrains [5-8]. On this basis, an auxiliary line parallel to the intersection line and the slope of the seabed to be measured is added to form the following figure. The 70-meter deep coverage range, denoted as D_{70}, is divided into two parts, K and L, for calculation. The newly divided shape is obtained and illustrated in Figure 1.

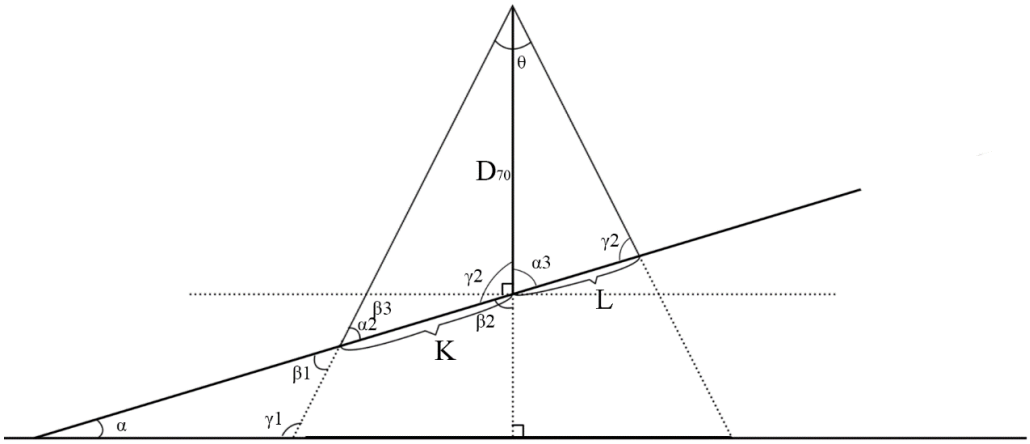

Figure 1: Two-dimensional schematic diagram of the cross-section of the sound wave and the slope of Haiti

It is already known that the slope angle α is 1.5 degrees, D is 70 meters, and the opening angle θ of the multi-beam transducer is 120 degrees. It is known that the angle γ_1 is 150 degrees. The complementary angle β_1 is calculated as $\pi - \alpha - \gamma_1$, which equals 28.5 degrees, and its vertical angle α_2 is 28.5 degrees. The length of K can be determined by the Law of Sines.

$$\frac{\sin\frac{\theta}{2}}{K} = \frac{\sin\alpha_2}{D_{70}}$$

$$\Rightarrow K = \frac{\sin\frac{\theta}{2}}{\sin\alpha_2} \cdot D_{70} = 127.0473 \tag{1}$$

And $\alpha_3 = 90° - \alpha = 88.5°$, $\gamma_3 = \pi - \frac{\theta}{2} - \alpha_3 = 31.5°$.The following reasoning is derived from the sinusoidal theorem

$$\frac{\sin\frac{\theta}{2}}{L} = \frac{\sin\gamma_3}{D_{70}}$$

$$\Rightarrow L = \frac{\sin\frac{\theta}{2}}{\sin\gamma_3} \cdot D_{70} = 116.0228 \tag{2}$$

At this point, the coverage width at a depth of 70 meters, denoted as W_{70}, is calculated to be $W_{70} = K + L = 243.0702$.

When the survey vessel moves 200 meters towards the shallower area, denoted as $d = 200$ meters, the water depth D_{200}, the coverage area W_{200}, and the overlap rate $\eta_{0\sim100}$ with the previous coverage area are unknown, as illustrated in Figure 2.

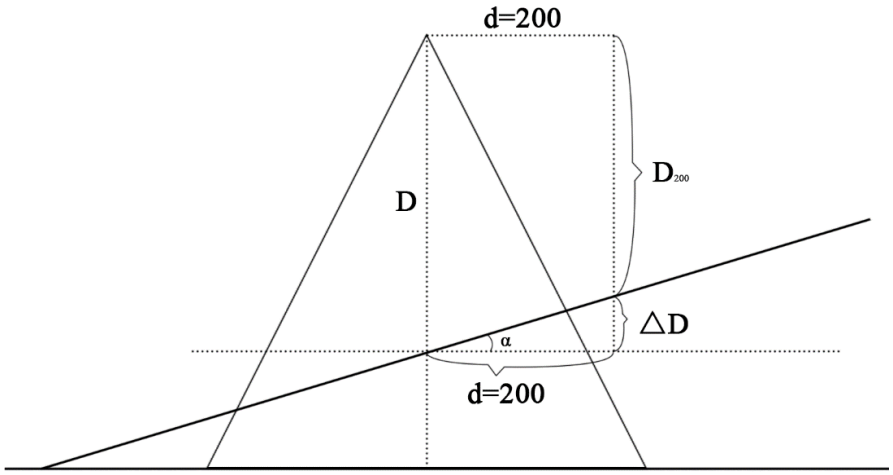

Figure 2: Schematic diagram of the unknown overlap range of adjacent lateral lines

From the diagram, it is easy to see that when $d > 0$, $D_{200} = D - \Delta D$, and conversely, $D_{-200} = D + \Delta D$. The following results are obtained using trigonometric functions.

$$\tan\alpha = \frac{\Delta D}{d}$$
$$\Rightarrow \Delta D = d \cdot \tan\alpha = 5.2371 \tag{3}$$

Then $D_{200} = D - \Delta D = 70 - 5.2372 = 64.7628$. Using the same method, this article can determine the sea depth when \(d \) equals different values. Subsequently, by applying the Law of Sines, this article can calculate the coverage area obtained by the survey vessel at each depth, as shown in Table 1.

Table 1: Coverage Width at Different Sea Depths

The distance from the survey line to the central point/m	-800	-600	-400	-200	0	200	400	600	800
Depth of the Sea/m	90.94	85.71	80.47	75.23	70.00	64.76	59.52	54.28	49.05
Coverage Width/m	315.81	297.62	279.44	261.25	243.07	224.88	206.69	188.51	170.32

At this point, the only remaining unknowns are the overlap rates between each survey line and the previous one. Taking the sideline at the origin and the sideline at D_{200} as an example, the coverage width at the origin can be divided into an overlapping part $\text{len}(\eta)$ and a remaining part t. As shown in Figure 3.

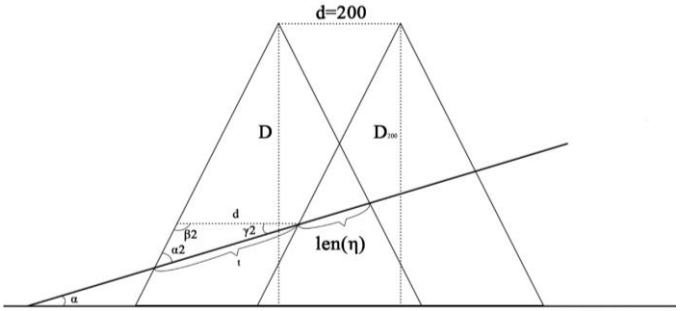

Figure 3: Schematic diagram Schematic diagram of the overlap range

When d is parallel to the diagram, a small triangle with t as its side is obtained. Knowing that $\alpha_2 = 28.5°$, $\gamma_3 = \alpha = 1.5°$, and $\beta_2 = \pi - \alpha_2 - \gamma_3$, then according to the Law of Sines, the following results are obtained.

$$\frac{\sin\beta_2}{t} = \frac{\sin\alpha_2}{d}$$
$$\Rightarrow t = \frac{\sin\beta_2}{\sin\alpha_2} \cdot d = 209.57 \tag{4}$$

Then $\mathrm{len}(\eta) = W_{70} - t = 33.4964$. The overlap rate formula $\eta = 1 - \frac{d}{w}$ given for flat seabed terrain does not apply to uneven seabed terrain [9]. In flat sea areas, the strip width between adjacent survey lines is the same, while in uneven sea areas, the strip widths are different. Therefore, the average width of two adjacent strips is taken to ensure the rigor of the overlap rate. After incorporating the change in angles, it is ultimately modified to

$$\eta = len(\eta)/(\frac{W_{x-1} + W_x}{2}) \tag{5}$$

Finally, the overlap rate of the two survey lines at the origin and the shallow part of the probe vessel is obtained $\eta_{0\sim200} = 33.4964/((243.0702 + 224.8844)/2) = 14.316$. In the same way, the overlap rate of the remaining part of the survey line can be obtained, as shown in Table 2.

Table 2: Overlap Rate Calculation Results (Results Retained to Two Decimal Places)

Measure the distance from the center point to the line/m	-800	-600	-400	-200	0	200	400	600	800
Depth of the Sea/m	90.94	85.71	80.47	75.23	70.00	64.76	59.52	54.28	49.05
Coverage Width/m	315.81	297.62	279.44	261.25	243.07	224.88	206.69	188.51	170.32
The overlap rate with the previous measuring line/%	——	34.63	30.51	25.84	20.49	14.31	7.09	-1.45	-11.73

3. Elliptical coverage area calculation for subsea multibeam measurements

The previous text mentioned that when a multi-beam transducer emits sonar waves in a fan shape to measure the smooth slope of the seabed, if it remains stationary and rotates a full circle, what is obtained is an elliptical area. In light of this, to obtain the multi-beam measurement model for the moving survey vessel under such conditions, we can project the movement of the survey vessel onto a polar coordinate system, calculate the strip width at each angle when the depth is different, which is calculating the width of the ellipse at different angles θ and different polar radii ρ in the polar coordinate system [10]. As shown in Figure 4.

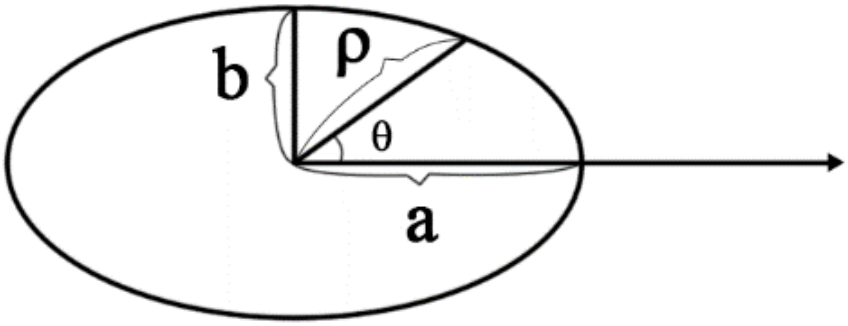

Figure 4: Schematic diagram of the measurement range of the multi-beam transducer at a slope

It is easy to understand that when $\beta = 0°$, the normal vector of the seabed slope is parallel to the projection of the measuring line, and at this time, the strip width W is equal to the short axis of the ellipse,2b. When $\beta = 90°$, the normal vector of the seabed slope is perpendicular to the projection of the measuring line, which is equivalent to the calculation of the model mentioned earlier, as shown in Figure 5.

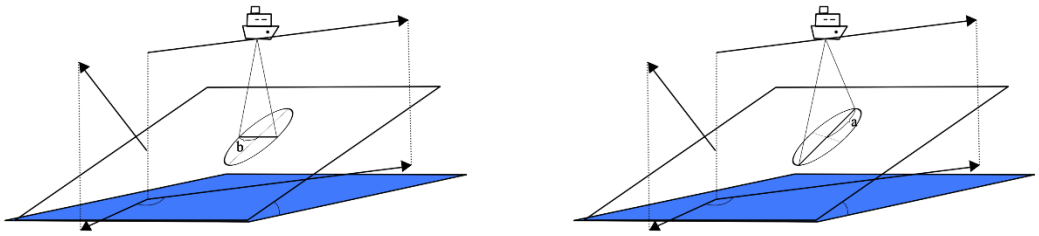

Figure 5: Schematic diagram of the long and short axes of the measurement range

When β equals 0 °, D equals 120 °, and θ equals 120 °, the relationship of trigonometric functions can be used to derive the minor axis b as $\frac{W}{2} = \frac{D}{\tan 30°}$. When β equals 90 °, D equals 120 °, and θ equals 120 °, the previous algorithm can be used to obtain the major axis a as $\frac{W}{2} = K + L$. As shown in Figure 6.

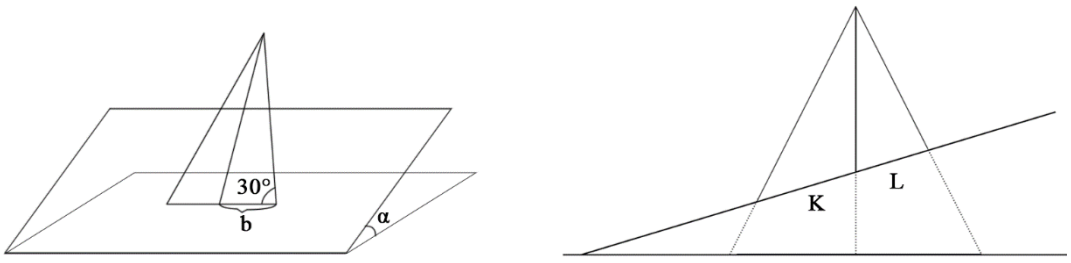

Figure 6: Schematic diagram of the length of the long and short axes

In actual problem-solving, the east-west direction often does not affect the values of a and b. The decisive factor is the length variable y in the north-south direction. When the angle of advance β and the number of nautical miles g are determined, it is easy to know that $y = g \cdot \cos\beta$. After the change, the water depth $D_{new} = D + \Delta D$, and it is easy to know from the trigonometric function that $\Delta D = y \cdot \tan\alpha$. Thus, all unknowns have been obtained. As shown in Figures 7 and 8.

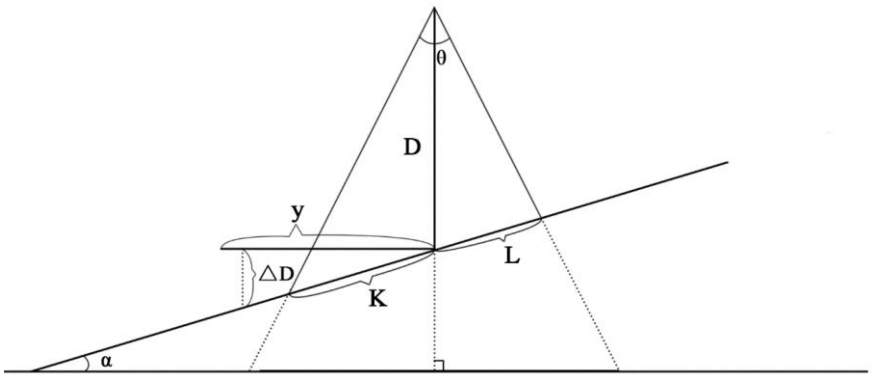

Figure 7: Schematic diagram of water depth change

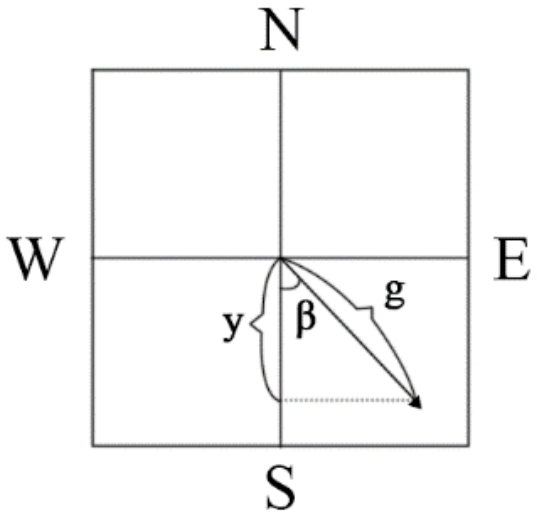

Figure 8: Schematic diagram of water depth change

A and B are organized as:

$$a = (D + g\cos\beta\tan\alpha)\cdot\sin 60°\cdot\left(\frac{1}{2\sin 31.5°} + \frac{1}{2\sin 28.5°}\right)$$
$$b = \frac{D + g\cos\beta\tan\alpha}{\tan\alpha} \tag{6}$$

The general equation for an ellipse is as follows:

$$\frac{x^2}{a^2} + \frac{y^2}{b^2} = 1 \tag{7}$$

After substituting the polar coordinate system, the polar coordinate equation of the ellipse can be obtained, and the following results can be solved:

$$\rho = \sqrt{\frac{a^2 b^2}{a^2\sin^2\beta + b^2\cos^2\beta}} \tag{8}$$

The width of the strip at each depth is $W = 2\rho$. The calculation result is calculated by substituting the relevant data, as shown in Table 3.

Table 3: Coverage width

Coverage width/m		nautical mile of the ship from the center point of the sea/Measure the distance							
		0	0.3	0.6	0.9	1.2	1.5	1.8	2.1
The angle between the direction of the measurement line/	0	415.69	466.09	516.48	566.88	617.28	667.68	718.08	768.48
	45	416.19	451.87	487.55	523.23	558.91	594.59	630.27	665.95
	90	416.69	416.69	416.69	416.69	416.69	416.69	416.69	416.69
	135	416.19	380.51	344.83	309.15	273.47	237.79	202.11	166.43
	180	415.69	365.29	314.89	264.49	214.09	163.69	113.29	62.90
	225	416.19	380.51	344.83	309.15	273.47	237.79	202.11	166.43
	270	416.69	416.69	416.69	416.69	416.69	416.69	416.69	416.69
	315	416.19	451.87	487.55	523.23	558.91	594.59	630.27	665.95

4. Conclusions

By abstracting real-world issues into geometric models, this paper proposes a calculation model for the coverage rate between adjacent strips and the coverage area of a single strip, taking into account the influence of different opening angles of multi-beam transducers and the continuous changes in seabed slope. This provides the basic conditions for the establishment of survey lines during ocean topographic scanning.

Firstly, under the conditions of the opening angle of the multi-beam transducer and the changing seabed slope, the problem of measuring the coverage width and the overlap rate of adjacent survey lines can be abstracted into a simple geometric model. By projecting the cross-section of the sound waves emitted by the multi-beam transducer onto the sea surface and intersecting with the seabed slope, an isosceles triangle is formed. On this basis, an imaginary line parallel to the intersection line is added on the seabed to be measured, dividing the isosceles triangle. Using trigonometric functions and the sine rule, the lengths of the sides and the angles of each of the divided smaller triangles are calculated one by one, ultimately resulting in the model.

Secondly, the method of the survey vessel's movement is to take the ocean's central point as the origin and start from different angles and distances to determine the strip width. This problem can be solved using the concept of the polar coordinate system. Additionally, when the survey vessel rotates 360 degrees at the same angle, an elliptical coverage area can be obtained on the seabed slope. By taking the two cases of $\beta=0°$ and $\beta=90°$ as the starting point, the general formula for the lengths of the major axis a and the minor axis b of the ellipse can be calculated, thus deriving the polar coordinate equation of the ellipse. Thereby, the strip width $W=2\rho$ can be determined. Further, the strip width after the survey vessel moves different nautical miles at different angles can be calculated.

This method provides a theoretical basis and computational approach for the establishment of survey lines in ocean topographic scanning, which helps to improve measurement efficiency and accuracy.

References

[1] Song Shuai, Zhou Yong, Zhang Kunpeng, Fan Xiaozhong. Review of high-precision and high-resolution underwater topography and geomorphology detection technology[J].Marine Development and Management,2019,36(06).

[2] WANG Xiaolin. A brief discussion on the application of multi-beam system in marine engineering survey[J].Science & Technology Information,2014,12(15).

[3] Hao Haoqi, Yao Chengzhang, Xie Min. Design of wide-bandwidth beam emission module[J].Acoustics and Electronic

Engineering,2024,(01).
[4] Wang Xiaohan, Hu Shuai, Lv Yang. Analysis of the application of NORBIT iWBMS integrated multi-beam sounding system in rapid survey of waterway[J]. China Water Transport, 2024,(03).
[5] Gong Xudong, Diao Xinyuan, Lv Yajun, et al. Application of Seabeam3012 in the topographic survey of Mariana seamount in the western Pacific Ocean[J].Marine Science,2020,44(08).
[6] LIU Lin. Causes and solutions of multi-beam bathymetry data distortion[J].Value Engineering,2023,42(21).
[7] Zheng Bozhen, Zhou Changjiang, Ge Juntao. Multi-beam marine topographic survey based on combined positioning technology [J].Standardization of Surveying and Mapping, 2022, 38(03).
[8] Yu Jiacheng, Jiang Kaiwen, Zhao Hongying. Neighborhood correction technology for the comprehensive effect of multi-beam bathymetry in terrain navigation[J].Global Positioning System,2023,48(06).
[9] ZHAO Zhanning. Research on geophysical interpretation method of complex seabed topography engineering [J].Value Engineering, 2024, 43(10).
[10] Xue Yang, Zhang Chao, Dong Yannan, et al. Seabed topographic survey based on multi-beam detection system [J].Science & Technology Information,2024,22(01).